International Journal of Computer Applications (0975 - 8887)
Volume 141 - No.2, May 2016

In Designing of ST-coded in-Home PLC Transmission Scheme

Hassan Mahasneh
Department of Communications Engineering
Tafila Technical University, Tafila, Jordan 66110

ABSTRACT

A new Multiple-Input Single-Output Powerline Communications (MISO PLC) transmission scheme is proposed as an extension to the conventional Single-Input Single-Output (SISO) PLC transmission scheme to achieve high data rate with diversity. This scheme is called Enhanced-PLC scheme (EPLC). A Space-Time (ST) coding is employed at the transmitter terminal. In addition, a modified Maximum-Likelihood (ML) decoder is proposed at the receiver over a quasi-static flat fading channel. The derivations of Signal-to-Noise Ratio (SNR), Symbol Error Rate (SER), outage probability, and spectral efficiency are conducted for the proposed PLC transmission scheme and compared to the conventional SISO and the 2×1 MISO ST-coded PLC schemes. The analytical results show that the proposed MISO PLC transmission scheme outperforms the SISO and the 2×1 MISO schemes in terms of error rate, outage probability, and rate performances.

Keywords

PLC, EPLC, In-home PLC Network, SISO, MISO, ST-Coding, ML Decoder

1. INTRODUCTION

The Power Line Communications (PLC) technology aims to deliver information via electrical power lines. Generally, PLC can be applied to all types of power line networks. Such networks are categorised according to the delivered voltage as: Ultra High Voltage (UHV), Extra High Voltage (EHV), High Voltage (HV), Medium Voltage (MV), and Low Voltage (LV) networks. LV networks are part of distribution stage that is commonly used for households via 230V single-phase.

In LV networks, or alternatively in-home networks, the single-phase electrical wiring is formed using three wires namely: Phase (P), Neutral (N), and Protective Earth (E). Such conductors are isolated by protective insulators. In case of conventional in-home PLC network, each conductor can carry information and therefore form a Single-Input Single-Output (SISO) PLC configuration. In the PLC literature, SISO PLC has been widely discussed such as in [10, 1, 8].

In contrast, the three conductors, P, N, and E, can be exploited for transmission, and therefore offers space diversity. The transmission from the three conductor to a single destination forms a Multiple-Input Single-Output (MISO) PLC configuration, or Multiple-Input Multiple-Output (MIMO) PLC configuration from the three conductors to multiple destinations. Such scenarios can be exploited to enhance PLC diversity, and therefore, reliable transmission is achieved. Recently MIMO for single phase in-home PLC has been reported [3, 7, 5]. Various STC techniques have been discussed in MIMO PLC configuration as in [6, 11, 12, 4].

In case of MISO PLC, Furukawa et. al. [2] investigated a MISO system for in-home PLC, based on OFDM and space-frequency codes. The authors use two-wire installations, however, in the fusion box, three wires are available which make MISO possible if the transmitter is located in the fuse box. Furthermore, de Campos et. al. [9] investigated a MISO access PLC system based on single carrier modulation. Most conducted research regarding 3×1 MISO PLC configuration consider three transmitting terminals that that are not simultaneously broadcasting. This could have an impact on the transmission rate.

In this paper a new MISO PLC scheme is proposed in order to achieve higher data rate transmission with diversity. This new scheme is called Enhanced-PLC (EPLC) scheme. EPLC is proposed for single-carrier modulation, so it targets narrowband applications. Moreover, a modified ML decoder is proposed for the EPLC scheme. The performance of the EPLC scheme is compared with the conventional SISO and the 2×1 ST-coded MISO PLC schemes.

This paper is organized as follows. Section 2.1 provides a brief description of the system model for the EPLC scheme. Section 2.2 presents the proposed modified ML decoder for the proposed EPLC scheme. Section 3 provides the performance analyses for the new scheme. Such analyses include: instantaneous SNR, SER, mutual information, achieved rate, and outage probability. Finally, Section 4 provides analytical and simulation results for the conventional SISO scheme, the 2×1 ST-coded MISO PLC scheme, and the proposed EPLC scheme.

2. A PROPOSED EPLC TRANSMISSION SCHEME

The PLC transmission scheme is proposed to increase data rate and improve the reliability of transmission between the transmitter and the receiver in an in-home PLC network. The scheme uses the three wires in at-home power network: the phase (P), the neutral (N), and the protected earth (E). Multiple-wires PLC communication is part of the MIMO PLC standard to enhance the desired transmitted signal and transmission capacity.

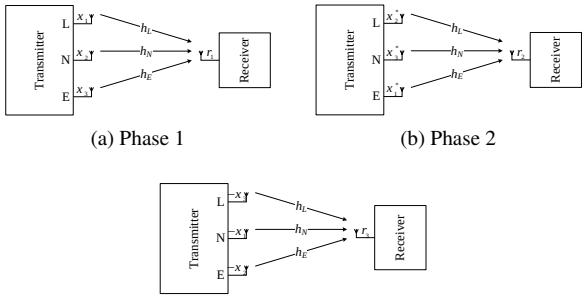

(a) Phase 1 (b) Phase 2

(c) Phase 3

Fig. 1: The Proposed 3×1 PLC Transmission (EPLC) Scheme Phases.

2.1 System Model

A 3×1 MISO PLC transmission scheme with three transmission phases is proposed for in-home PLC-wireless networks. In all phases, terminals transmit signals through orthogonal channels by using TDMA. The proposed EPLC scheme targets downlink transmissions where the data source terminal transmits information to the receiver, as shown in Fig. 1. The transmitter is assumed be equipped with three transmit antennas, while the receiver is equipped with single receive antenna. Therefore, a 3×1 MISO configuration is formed. Moreover, different phase wires are assumed perfectly isolated and uncoupled.

Table 1. : Transmission Schedule For Each PLC Antenna Terminal

Phase	**Phase** (P)	**Neutral** (N)	**Protective Earth** (E)
Phase 1	Broadcasts x_1	Broadcasts x_2	Broadcasts x_3
Phase 2	Broadcasts x_2^*	Broadcasts x_3^*	Broadcasts x_1^*
Phase 3	Broadcasts $-x_3$	Broadcasts $-x_1$	Broadcasts $-x_2$

At the transmitter, the information bit sequence is first mapped from a complex signal constellation into a complex symbol sequence. The complex symbol sequence is then parsed into code vectors $\mathbf{s} \triangleq \begin{bmatrix} x_1 & x_2 & x_3 \end{bmatrix}^T$. It is assumed that the channel coherence time is comparable to the symbol duration due to relative motion between transmitter and receiver. The channel between any transmit and receive antenna is modelled as uncorrelated frequency-flat but time-selective Rayleigh fading. The channel gains are assumed time-invariant within three signalling intervals but may vary between every three signalling intervals. The transmitted power from each transmit antenna is assumed identical and equals P.
The downlink transmission to the receiver is accomplished in three phases as illustrated in Fig. 1. In phase 1, the transmitter broadcasts the symbols x_1, x_2, and x_3 from the code vector via the first, the second, and third transmit antennas, respectively, as shown in Fig. 1 (a). The received signal at the receiver is written as

$$r_1 = \sqrt{P}\,(h_P x_1 + h_N x_2 + h_E x_3) + n_1 \tag{1}$$

where $h_P \sim CN(0, \sigma_P^2)$ is the channel coefficient from the first transmit antenna to the receiver, $h_N \sim CN(0, \sigma_N^2)$ is the channel coefficient from the second transmit antenna to the receiver, $h_E \sim CN(0, \sigma_E^2)$ is the channel coefficient from the third transmit antenna to the receiver, and $n_1 \sim CN(0, \sigma_{n_1}^2)$ is additive white Gaussian noise (AWGN).

In phase 2, Fig. 1 (b), the transmitter conjugates the data symbols and broadcasts it such that, the first, the second, and third transmit antennas transmit the symbols x_2^*, x_3^*, and x_1^*, respectively. The combined received signal at the receiver in phase 2 is written as

$$r_2 = \sqrt{P}\,(h_P x_2^* + h_N x_3^* + h_E x_1^*) + n_2 \tag{2}$$

where $n_2 \sim CN(0, \sigma_{n_2}^2)$ is AWGN. In phase 3, Fig. 1 (c), the transmitter broadcasts the symbols $-x_3$, $-x_1$, and $-x_2$ from the code vector through the first, the second, and the third transmit antennas, respectively. Therefore, the signal received at the receiver in phase 3 can be written as

$$r_3 = -\sqrt{P}\,(h_P x_3 + h_N x_1 + h_E x_2) + n_3 \tag{3}$$

where $n_3 \sim CN(0, \sigma_{n_3}^2)$ is AWGN. The three-phase transmission is carried on until the end of the entire symbol sequence. Assuming the channel conditions for all links in all phases are quasi-static over three consecutive signaling intervals, equations (1), (2), and (3) are combined in matrix form as

$$\begin{bmatrix} r_1 \\ r_2 \\ r_3 \end{bmatrix} = \sqrt{P} \begin{bmatrix} x_1 & x_2 & x_3 \\ x_2^* & x_3^* & x_1^* \\ -x_3 & -x_1 & -x_2 \end{bmatrix} \begin{bmatrix} h_P \\ h_N \\ h_E \end{bmatrix} + \begin{bmatrix} n_1 \\ n_2 \\ n_3 \end{bmatrix} \tag{4}$$

Taking the conjugate of r_2 in (2), equation (4) can be rewritten as

$$\underbrace{\begin{bmatrix} r_1 \\ r_2^* \\ r_3 \end{bmatrix}}_{\triangleq \mathbf{r}} = \sqrt{P} \underbrace{\begin{bmatrix} h_P & h_N & h_E \\ h_N^* & h_E^* & h_P^* \\ -h_E & -h_P & -h_N \end{bmatrix}}_{\triangleq \mathbf{H}} \underbrace{\begin{bmatrix} x_1 \\ x_2 \\ x_3 \end{bmatrix}}_{\triangleq \mathbf{x}} + \underbrace{\begin{bmatrix} n_1 \\ n_2^* \\ n_3 \end{bmatrix}}_{\triangleq \mathbf{n}} \tag{5}$$

where $\mathbf{r} \in C^{3\times 1}$ is the received signal vector, $\mathbf{H} \in C^{3\times 3}$ is the channel matrix, $\mathbf{x} \in C^{3\times 1}$ is the information code vector, and $\mathbf{n} \in C^{3\times 1}$ is the noise vector. It is clearly seen that the EPLC transmission scheme provides a transmission of three ST-coded symbols over three phases, or signaling intervals, and provides diversity for all transmitted symbols. In the following, a modified maximum-likelihood (ML) decoder is proposed to decode $\mathbf{r}$ over quasi-static fading channels.

2.2 Modified ML Decoder of EPLC Transmission Scheme Over Quasi-Static Fading Channel

Under the assumption of perfect channel state information (CSI) at the receiver, the conventional ML decoder [13] selects the code vector $\hat{\mathbf{x}} \triangleq \begin{bmatrix} \hat{x}_1 & \hat{x}_2 & \hat{x}_3 \end{bmatrix}^T$ according to

$$\hat{\mathbf{x}} = \arg\min_{\mathbf{x}} \|\mathbf{r} - \mathbf{H}\mathbf{x}\|^2 \tag{6}$$

where $\|..\|^2$ is the norm-squared operation. This is conventionally performed by multiplying the received signals in (5) by the conjugate transpose of the channel matrix to decouple the received symbols if the product of $\mathbf{H}^H$ and $\mathbf{H}$ is a diagonal matrix, i.e.

$$\underbrace{\mathbf{H}^H \mathbf{r}}_{\triangleq \hat{\mathbf{r}}} = \mathbf{H}^H \mathbf{H}\mathbf{x} + \underbrace{\mathbf{H}^H \mathbf{n}}_{\triangleq \hat{\mathbf{n}}}$$

and consequently, conventional ML decoding is used by computing the decision statistic vector $\hat{\mathbf{r}} \triangleq \begin{bmatrix} \hat{r}_1 & \hat{r}_2 & \hat{r}_3 \end{bmatrix}^T$ as

$$\hat{\mathbf{r}} \triangleq \mathbf{H}^H \mathbf{r} = (\zeta_1, \zeta_2, \zeta_3)\, \mathbf{I}_3 \hat{\mathbf{x}} + \hat{\mathbf{n}}$$

where ζ_1, ζ_2, and ζ_3 are complex-valued coefficients, and $\mathbf{I_3}$ is a 3×3 identity matrix. Equation (6) can be simplified as

$$\hat{\mathbf{x}}=\arg\min_{\mathbf{x}} \|\hat{\mathbf{r}}-(\zeta_1,\zeta_2,\zeta_3)\,\mathbf{I}_3\mathbf{x}\|^2$$

Consider the channel matrix $\mathbf{H}$ in (5). Assuming the channel to be time-invariant over three consecutive signaling periods, multiplying $\mathbf{H}$ by its conjugate transpose $\mathbf{H}^H$ yields,

$$\mathbf{H}^H\mathbf{H}=\begin{bmatrix} h_P^* & h_N & -h_E^* \\ h_N^* & h_E & -h_P^* \\ h_E^* & h_P & -h_N \end{bmatrix}\begin{bmatrix} h_P & h_N & h_E \\ h_N^* & h_E^* & h_P^* \\ -h_E & -h_P & -h_N \end{bmatrix}= \begin{bmatrix} |h_P|^2+|h_N|^2+|h_E|^2 & h_P^*h_N+h_E^*(h_P+h_N) & h_E^*h_N+h_P^*(h_N+h_E) \\ h_P^*h_E+h_N^*(h_P+h_E) & |h_P|^2+|h_N|^2+|h_E|^2 & h_N^*h_E+h_P^*(h_N+h_E) \\ h_E^*h_P+h_N^*(h_P+h_E) & h_N^*h_P+h_E^*(h_P+h_N) & |h_P|^2+|h_N|^2+|h_E|^2 \end{bmatrix} \quad (7)$$

The matrix obtained from multiplying $\mathbf{H}$ by its conjugate transpose $\mathbf{H}^H$ in (7) is not diagonal. Therefore, ML decoding of the received signals is degraded due to the non-zero off-diagonal terms. In this case, the conventional ML decoder in (7) is no longer valid. In this paper, a modified ML method is proposed where a matrix $\boldsymbol{\eta}$ is constructed such that its product with $\mathbf{H}$ is a diagonal matrix. i.e.

$$\boldsymbol{\eta}\mathbf{H}=diag\,(\zeta_1,\zeta_2,\zeta_3)\triangleq\zeta$$

where ζ_1, ζ_2, and ζ_3 are in general complex-valued coefficients that are specified later in this section. Define a 3×3 matrix $\boldsymbol{\eta}$

$$\boldsymbol{\eta}\triangleq\begin{bmatrix} \eta_1 & \eta_2 & \eta_3 \\ \eta_4 & \eta_5 & \eta_6 \\ \eta_7 & \eta_8 & \eta_9 \end{bmatrix}$$

Multiplying $\mathbf{H}$ by $\boldsymbol{\eta}$ yields

$$\begin{bmatrix} \eta_1h_P+\eta_2h_N^*-\eta_3h_E & \eta_1h_N+\eta_2h_E^*-\eta_3h_L & \eta_1h_E+\eta_2h_P^*-\eta_3h_N \\ \eta_4h_P+\eta_5h_N^*-\eta_6h_E & \eta_4h_N+\eta_5h_E^*-\eta_6h_L & \eta_4h_E+\eta_5h_P^*-\eta_6h_N \\ \eta_7h_P+\eta_8h_N^*-\eta_9h_E & \eta_7h_N+\eta_8h_E^*-\eta_9h_L & \eta_7h_E+\eta_8h_P^*-\eta_9h_N \end{bmatrix}$$

In order to diagonalize the product, the elements of $\boldsymbol{\eta}$ are selected to annihilate the off-diagonal terms. That is,
$\eta_4h_P+\eta_5h_N^*-\eta_6h_E=0$, $\eta_7h_P+\eta_8h_N^*-\eta_9h_E=0$,
$\eta_1h_N+\eta_2h_E^*-\eta_3h_P=0$, $\eta_7h_N+\eta_8h_E^*-\eta_9h_P=0$,
$\eta_1h_E+\eta_2h_P^*-\eta_3h_N=0$, and $\eta_4h_E+\eta_5h_P^*-\eta_6h_N=0$.
A set of values of η_1, η_2, η_3, η_4, η_5, η_6, η_7, η_8, and η_9 that satisfy the above equations can be obtained using numerical methods as, $\eta_1=|h_P|^2-h_E^*h_N$, $\eta_2=h_N^2-h_Ph_E$, $\eta_3=|h_E|^2-h_P^*h_N$, $\eta_4=|h_N|^2-h_P^*h_E$, $\eta_5=h_E^2-h_Ph_N$, $\eta_6=|h_P|^2-h_N^*h_E$, $\eta_7=|h_E|^2-h_N^*h_P$, $\eta_8=h_P^2-h_Nh_E$, and $\eta_9=|h_N|^2-h_E^*h_P$. Using the above values, $\boldsymbol{\eta}$ is written as

$$\boldsymbol{\eta}=\begin{bmatrix} |h_P|^2-h_E^*h_N & h_N^2-h_Ph_E & |h_E|^2-h_P^*h_N \\ |h_N|^2-h_P^*h_E & h_E^2-h_Ph_N & |h_P|^2-h_N^*h_E \\ |h_E|^2-h_N^*h_P & h_P^2-h_Nh_E & |h_N|^2-h_E^*h_P \end{bmatrix}$$

Establishing $\boldsymbol{\eta}$, the term $\boldsymbol{\eta}\mathbf{H}=diag\,(\zeta_1,\zeta_2,\zeta_3)\triangleq\boldsymbol{\zeta}$ is a diagonal matrix with diagonal terms given by ζ_1, ζ_2, and ζ_3, respectively. That is,

$$\zeta_1=\zeta_2=\zeta_3\triangleq\zeta=h_P^*\left(h_P^2-h_Nh_E\right)+h_N^*\left(h_N^2-h_Ph_E\right)+h_E^*\left(h_E^2-h_Ph_N\right)$$

The decision statistic vector $\hat{\mathbf{r}}$ for the modified ML decoder is given by

$$\underbrace{\begin{bmatrix}\hat{r}_1\\ \hat{r}_2\\ \hat{r}_3\end{bmatrix}}_{\hat{\mathbf{r}}}=\sqrt{P}\underbrace{\begin{bmatrix}\zeta & 0 & 0\\ 0 & \zeta & 0\\ 0 & 0 & \zeta\end{bmatrix}}_{\boldsymbol{\zeta}}\underbrace{\begin{bmatrix}x_1\\ x_2\\ x_3\end{bmatrix}}_{\mathbf{x}}+\underbrace{\begin{bmatrix}\hat{n}_1\\ \hat{n}_2\\ \hat{n}_3\end{bmatrix}}_{\hat{\mathbf{n}}} \quad (8)$$

where $\hat{\mathbf{r}}\triangleq\boldsymbol{\eta}\mathbf{r}$ and $\hat{\mathbf{n}}\triangleq\boldsymbol{\eta}\mathbf{n}$. The decoding of $\hat{\mathbf{x}}$ is then performed as

$$\hat{\mathbf{x}}=\arg\min_{\mathbf{x}} \|\hat{\mathbf{r}}-\boldsymbol{\zeta}\mathbf{x}\|^2$$

3. PERFORMANCE ANALYSIS

In this section, we present the analyses of SNR, SER, and other performance analyses for the proposed EPLC transmission scheme using M-ary phase shift keying (MPSK) modulation.

3.1 Instantaneous Signal-to-Noise Ratio (SNR) Analysis

In this section, an instantaneous SNR expression is derived for the proposed EPLC transmission scheme. According to (8), the noise vector $\hat{\mathbf{n}}\triangleq\begin{bmatrix}\hat{n}_1 & \hat{n}_2 & \hat{n}_3\end{bmatrix}^T$ is expressed as

$$\hat{\mathbf{n}}\triangleq\underbrace{\begin{bmatrix} |h_P|^2-h_E^*h_N & h_N^2-h_Ph_E & |h_E|^2-h_P^*h_N \\ |h_N|^2-h_P^*h_E & h_E^2-h_Ph_N & |h_P|^2-h_N^*h_E \\ |h_E|^2-h_N^*h_P & h_P^2-h_Nh_E & |h_N|^2-h_E^*h_P \end{bmatrix}}_{\boldsymbol{\eta}}\underbrace{\begin{bmatrix}n_1\\ n_2^*\\ n_3\end{bmatrix}}_{\mathbf{n}}= \begin{bmatrix} n_1\left(|h_P|^2-h_E^*h_N\right)+n_2^*\left(h_N^2-h_Ph_E\right)+n_3\left(|h_E|^2-h_P^*h_N\right) \\ n_1\left(|h_N|^2-h_P^*h_E\right)+n_2^*\left(h_E^2-h_Ph_N\right)+n_3\left(|h_P|^2-h_N^*h_E\right) \\ n_1\left(|h_E|^2-h_N^*h_P\right)+n_2^*\left(h_P^2-h_Nh_E\right)+n_3\left(|h_N|^2-h_E^*h_P\right) \end{bmatrix}$$

where $\hat{n}_1$, $\hat{n}_2$, and $\hat{n}_3$ are modeled as a zero-mean, conditionally complex Gaussian random variables with variances (assuming h_P, h_N, and h_E are fixed)

$$\sigma^2_{\hat{n}_1}(\mathbf{H})=\sigma^2_{n_1}\left||h_P|^2-h_E^*h_N\right|^2+\sigma^2_{n_2}\left|h_N^2-h_Ph_E\right|^2+\sigma^2_{n_3}\left||h_E|^2-h_P^*h_N\right|^2,$$

$$\sigma^2_{\hat{n}_2}(\mathbf{H})=\sigma^2_{n_1}\left||h_N|^2-h_P^*h_E\right|^2+\sigma^2_{n_2}|h_E^2-h_Ph_N|^2+\sigma^2_{n_3}\left||h_P|^2-h_N^*h_E\right|^2,$$

and

$$\sigma^2_{\hat{n}_3}(\mathbf{H})=\sigma^2_{n_1}\left||h_E|^2-h_N^*h_P\right|^2+\sigma^2_{n_2}\left|h_P^2-h_Nh_E\right|^2+\sigma^2_{n_3}\left||h_N|^2-h_E^*h_P\right|^2,$$

respectively. With knowledge of the channel coefficients h_P, h_N, and h_E at the receiver, the conditional SNRs, Γ_1, Γ_2, and Γ_3, at the output of the decoder are given by

$$\Gamma_1(\mathbf{H})=\frac{|\zeta|^2}{\sigma^2_{\hat{n}_1}(\mathbf{H})}= =\frac{P\left(|h_P|^2\left|h_P^2-h_Nh_E\right|^2+|h_N|^2\left|h_N^2-h_Ph_E\right|^2+|h_E|^2\left|h_E^2-h_Ph_N\right|^2\right)}{\sigma^2_{n_1}\left||h_P|^2-h_E^*h_N\right|^2+\sigma^2_{n_2}\left|h_N^2-h_Ph_E\right|^2+\sigma^2_{n_3}\left||h_E|^2-h_P^*h_N\right|^2},$$

$$\Gamma_2(\mathbf{H})=\frac{|\zeta|^2}{\sigma^2_{\hat{n}_2}(\mathbf{H})}= =\frac{P\left(|h_P|^2\left|h_P^2-h_Nh_E\right|^2+|h_N|^2\left|h_N^2-h_Ph_E\right|^2+|h_E|^2\left|h_E^2-h_Ph_N\right|^2\right)}{\sigma^2_{n_1}\left||h_N|^2-h_P^*h_E\right|^2+\sigma^2_{n_2}\left|h_E^2-h_Ph_N\right|^2+\sigma^2_{n_3}\left||h_P|^2-h_N^*h_E\right|^2},$$

and

$$\Gamma_3(\mathbf{H}) = \frac{|\zeta|^2}{\sigma^2_{\hat{n}_3}(\mathbf{H})} = \frac{P\left(|h_P|^2\left|h_P^2 - h_N h_E\right|^2 + |h_N|^2\left|h_N^2 - h_P h_E\right|^2 + |h_E|^2\left|h_E^2 - h_P h_N\right|^2\right)}{\sigma^2_{n_1}\left||h_E|^2 - h_N^* h_P\right|^2 + \sigma^2_{n_2}\left|h_P^2 - h_N h_E\right|^2 + \sigma^2_{n_3}\left||h_N|^2 - h_E^* h_P\right|^2}$$

respectively, and the instantaneous overall conditional SNR is given by

$$SNR(\mathbf{H}) = \Gamma_1(\mathbf{H}) + \Gamma_2(\mathbf{H}) + \Gamma_3(\mathbf{H}) \quad (9)$$

3.2 SER Analysis for MPSK

For an uncoded system with MPSK modulation (M = 2^i, i = 1, 2, ...), the SER is given by [13]

$$SER_{MPSK}(\mathbf{H}) \triangleq 2Q\left[\sqrt{2SNR(\mathbf{H})}\sin\left(\frac{\pi}{M}\right)\right] \quad (10)$$

where Q[.] is the Q-function. Here, the exact instantaneous SER is obtained by using the actual instantaneous SNR in (9).

3.3 Other Performance Measures: Mutual Information, Achieved Rate, and Outage Probability

In this section, the mutual information, the achieved channel rate, and the outage probability are derived for the EPLC transmission scheme. The mutual information is a measure of the reliability of communications between communicating terminals. The mutual information [13] for the proposed EPLC transmission scheme in terms of the channel fades can be given as

$$I = \frac{1}{2}\log_2(1 + SNR(\mathbf{H}))$$

Using the expression of the overall *SNR*(**H**) in (9) yields,

$$I = \frac{1}{2}\log_2(1 + \Gamma_1(\mathbf{H}) + \Gamma_2(\mathbf{H}) + \Gamma_3(\mathbf{H}))$$

The outage probability for the proposed EPLC transmission scheme is defined as the probability that the mutual information between terminals is less than the channel rate R [13]. Hence, the outage event is equivalent to

$$\Pr[I < R] = \Pr\left[(\Gamma_1(\mathbf{H}) + \Gamma_2(\mathbf{H}) + \Gamma_3(\mathbf{H})) < 2^{2R} - 1\right]$$

4. RESULTS

4.1 The SER Performance for the Proposed EPLC Scheme

In order to demonstrate the benefits of employing the proposed EPLC scheme over the conventional SISO and the 2×1 ST-coded PLC schemes, the analytical and simulated SER versus SNR are plotted as shown in Fig.2. The analytical curves are obtained for systems employing QPSK modulation. The channel coefficients, h_P, h_N, and h_E, are modelled as zero-mean, complex Gaussian random variables with variances of σ_P^2=1, σ_N^2=0.9, and σ_E^2=0.8, respectively. For each channel realization, the instantaneous SNR is calculated using (9) and averaged over the number of channel realizations. Then, (10) is used to find the analytical average SER. On the other hand, the simulated curves are obtained by generating 1×10^7 Rayleigh fading channel realizations for h_P, h_N, and h_E with variances of σ_P^2=1, σ_N^2=0.9, and σ_E^2=0.8, respectively. Also, 1×10^7 data symbols are generated, mapped, and transmitted according to the proposed EPLC scheme. The received symbols are then decoded according to the modified ML decoder. Finally, the symbol error rate is calculated by counting the number of corrupted symbols and comparing it to the total number of transmitted symbols. Fig. 2 shows that the proposed scheme significantly outperforms the conventional SISO and the 2×1 PLC schemes. For example, at an SER of 4×10^{-3}, the SNR requirement of the EPLC scheme is approximately 3dB lower than for the 2×1 scheme, and approximately 9dB lower than for the SISO scheme. Moreover, the simulated SER curves match the analytical curves very well.

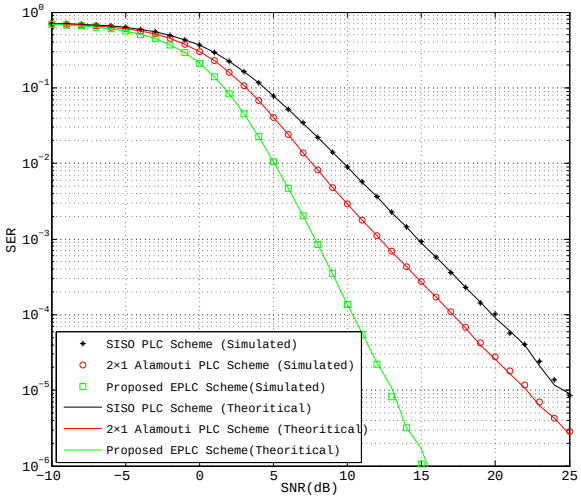

Fig. 2: SER comparison for the conventional SISO, the 2×1 ST-coded, and the proposed EPLC schemes.

4.2 The Outage Probability Performance of the Proposed EPLC Scheme

Fig. 3 illustrates the outage probability versus SNR for the proposed EPLC scheme over the conventional SISO and the 2×1 ST-coded PLC schemes. The outage probability is evaluated for each scenario as a function of the SNR at a fixed spectrum efficiency of 2bps/Hz. The figure shows that the outage probability is high for poor link strength and decays for all scenarios whenever the link strength improves. The EPLC scheme shows the lowest outage probability followed by the 2×1 ST-coded PLC scheme while the worst of all is the conventional SISO scheme. For example, at 15dB SNR, the outage probability for proposed scheme is 2×10^{-4}, for the 2×1 ST-coded PLC scheme is 4×10^{-3}, and for the conventional SISO is 1.5×10^{-3}. This is an improvement of approximately two orders of magnitude over the conventional SISO scheme.

4.3 The Spectral Efficiency Performance of the Proposed EPLC Scheme

Fig. 4 illustrates the outage probability versus spectral efficiency (bps/Hz) for the EPLC scheme, the conventional SISO scheme, and the 2×1 scheme. The outage probability is evaluated for each scenario as a function of the spectral efficiency at a fixed SNR of 15dB. The figure shows that the outage probability increases with the spectral efficiency. The proposed PLC scheme shows the least outage probability when increasing the spectral efficiency.

5. CONCLUSIONS

In this paper, the performance of a new 3×1 MISO PLC transmission was proposed and investigated. The scheme aims for single-carrier modulation and narrowband applications. Based on the system and the received signal model of the proposed scheme, a modified ML decoder is proposed to recover the received symbols over a quasi-static fading channel. In addition, the analysis of the SNR, SER, mutual information, the achieved rate, and the outage probability were conducted and compared to the conventional SISO and the 2×1 PLC schemes. The results showed significant improvement for the proposed scheme over the conventional SISO and the 2×1 PLC schemes in terms of SER. Also, the results showed higher transmission rate and lower outage probability are achieved when employing the proposed scheme than the the conventional SISO and the 2×1 PLC schemes.

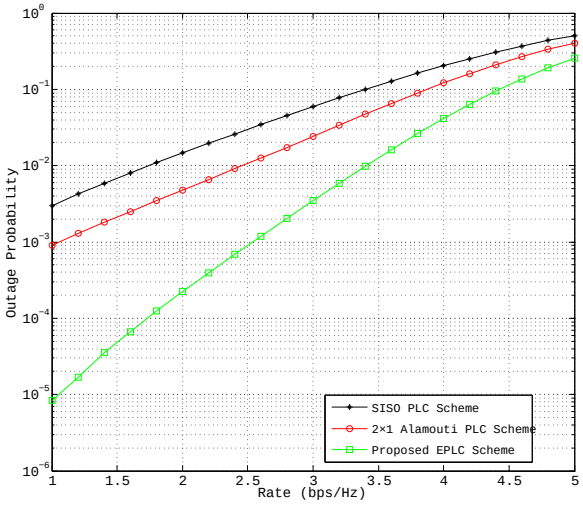

Fig. 3: P_{out} versus SNR for the proposed EPLC scheme, the conventional SISO scheme, and the 2×1 scheme assuming spectral efficiency = 2bps/Hz

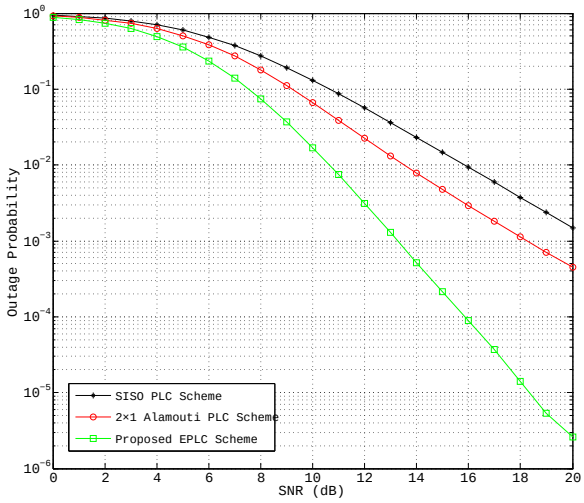

Fig. 4: P_{out} versus spectral efficiency for the proposed MISO scheme, the conventional SISO scheme, and the 2×1 scheme assuming SNR = 15dB

6. REFERENCES

[1] DAlessandro, A. M. Tonello, and L. Lampe. Adaptive pulse-shaped ofdm with application to in-home power line communications. *Telecommunications Systems Journal*, 51(1):3–13, 2011.

[2] F. de Campos, R. Machado, M. Ribeiro, and M. de Campos. Miso single-carrier system with feedback channel information for narrowband plc applications. *International Symposium on Power Line Communications and Its Applications*, page 301306, 2009.

[3] T. Esmailian, F. R. Kschischang, and P. G. Gulak. In-building power lines as high-speed communication channels: Channel characterization and a test channel ensemble. In *International Journal of Communication Systems*, volume 16, pages 381–400, 2003.

[4] C. Giovaneli, B. Honary, and P. Farrell. Spacefrequency coded ofdm system for multi-wire power line communications. *International Symposium on Power Line Communications and Its Applications*, 20(3):191195, 2005.

[5] C. L. Giovaneli, P. G. Farrell, and B. Honary. International symposium on power line communications and its applications. *Information Theory, IEEE Transactions on*, pages 50–55, 2003.

[6] C. L. Giovaneli, B. Honary, and P. G. Farrell. Optimum space-diversity receiver for class a noise channels. *International Symposium on Power Line Communications and Its Applications*, pages 189–194, 2004.

[7] C. L. Giovaneli, P. F. J. Yazdani, and B. Honary. Application of spacetime diversity/coding for power line channels. *International Symposium on Power Line Communications and Its Applications*, pages 101–105, 2002.

[8] Ferreira H.C., L. Lampe, J. Newbury, and T.G. Swart. *Power Line Communications: Theory and Applications for Narrowband and Broadband Communications over Power Lines*. New York. Wiley and Sons, 2010.

[9] M. Kuhn, D. Benyoucef, and A. Wittneben. Linear block codes for frequency selective plc channels with colored noise and multiple narrowband interference. *Vehicular Technology Conference, VTC Spring 2002*, page 17561760, 2002.

[10] Y. Ma, K. Liu, Z. Zhang, J. Yu, and X. Gong. Modeling the colored background noise of power line communication channel based on artificial neural network. *Wireless and Optical Communications Conference*, 2010.

[11] A. Papaioannou, G. D. Papadopoulos, and F.N. Pavlidou. Performance of spacetime block coding over the power line channel in comparison with the wireless channel. *International Symposium on Power Line Communications and Its Applications*, pages 362–366, 2004.

[12] A. Papaioannou, G. D. Papadopoulos, and F.N. Pavlidou. Performance of spacetime block coding in powerline and satellite communications. *J. Commun. Inf. Syst.*, 20(3):174–181, 2005.

[13] J.G. Proakis and M. Salehi. *Digital Communications*. McGraw-Hill International Edition. McGraw-Hill, 2008.